

**Thermal-hydraulic Calculations for the
GRR-1 Research Reactor Core Conversion
to Low Enriched Uranium Fuel**

C. Housiadas

*National Centre for Scientific Research “Demokritos”
Institute of Nuclear Technology and Radiation Protection
P.O. Box 60228, 15310 Agia Paraskevi, Athens, Greece*

Abstract – *The Research Reactor Laboratory has been equipped with the thermal-hydraulic codes PLTEMP, NATCON and PARET to assess the safety issues of the GRR-1 reactor core conversion to Low Enriched Uranium (LEU) fuel. The codes are used to carry out both steady-state and transient analyses of safety margins and limits. The steady-state analysis is made for both forced and natural convection cooling. The transient analysis is made for assessing relevant accident sequences, including reactivity accidents and loss-of-flow accidents. The results of the simulations show that LEU fuel promotes reactor safety, because of the enhancement of the reactor feedback mechanisms.*

Keywords: *Thermal-hydraulics, Reactor Safety, LEU fuel, Research Reactors, GRR-1.*

**December 1999
(Revised in September 2000)**

TABLE OF CONTENTS

1	INTRODUCTION	3
2	AVAILABLE CODES	3
2.1	Code PLTEMP	3
2.2	Code NATCON	3
2.3	Code PARET	4
3	STEADY-STATE CALCULATIONS	4
3.1	Calculation of safety limits in the forced convection mode	4
3.2	Calculation of safety limits in the natural convection mode	5
4	TRANSIENT CALCULATIONS	5
4.1	Reactor Model	6
4.2	Simulation of maximum start-up accident	6
4.3	Simulation of maximum reactivity insertion accident	7
4.4	Simulation of maximum loss-of-flow accident	8
4.5	Simulation of partial loss-of-flow accident	10
5	ANALYSIS OF LOSS-OF-COOLANT ACCIDENT	10
5.1	Calculation of pool draining	10
5.2	Calculation of natural convection in air	11
5.2.1	<i>Fission product decay heat</i>	11
5.2.2	<i>Physical model</i>	11
5.3	Results	13
6	CONCLUSIONS	13
7	REFERENCES	14

1 INTRODUCTION

The “Demokritos” research reactor GRR-1 (Greek Research Reactor-1) is a typical pool-type reactor with plate-type fuel elements, in operation since the early sixties at the Institute of Nuclear Technology and Radiation Protection (INPTA). In line with the worldwide campaign of converting research reactor cores from HEU (Highly Enriched Uranium) fuel to LEU (Low Enriched Uranium) fuel, the reactor has been recently fuelled with LEU elements of U_3Si_2 -Al type. This conversion entailed an up-dated safety assessment and thermal-hydraulic analysis. The thermal-hydraulic analysis of the original HEU core has been performed with the code THEAP, a software capability purposely developed in house in mid-eighties [1]. The results of this early assessment have been accommodated in the first Safety Analysis Report made for the original HEU core [2]. In response to the calculational needs stemming from the core conversion, new capabilities have been built, tested and implemented at the Research Reactor Laboratory.

The objective of the present report is two-fold. First, to give an account of the thermal-hydraulic codes that are now available at the Research Reactor Laboratory of INPTA Institute. Second, to present the results of the various calculations that have been performed to support the safety assessment of the new core. As it will become apparent, the available codes fulfil satisfactorily the GRR-1 operational needs, as required for performing thermal-hydraulic assessments on a routine basis.

2 AVAILABLE CODES

Three codes are available for carrying out thermal-hydraulic calculations, namely, PARET, PLTEMP, and NATCON. All three have been provided by Argonne National Laboratory (ANL), and have been installed on a PC. The codes are in FORTRAN and their source is available. Although the executables have been provided, the installation on the PC was made from the source. This entailed a number of modifications to resolve compatibility issues with respect to the local platform characteristics (compiler, file location etc.). Currently, all three codes are operational.

The codes PLTEMP and NATCON are used for steady-state calculations. The former is employed for forced convection cases and the latter is employed for natural convection cases. The code PARET is used for investigating transient cases. Below, a brief outline of each code is given.

2.1 Code PLTEMP

The code PLTEMP [3] calculates for steady-state forced convection conditions the flow velocity, fuel plate temperature, coolant temperature, as well as the margins to boiling crisis and flow instability. The core can be described either via a single hot channel associated with a single hot plate, or via the so-called subchannel description. In the latter case, the core is described by a cluster of parallel, non interacting channels connecting two plena, which can have different characteristics. The subchannel description can accommodate up to 150 fuel elements with up to 30 channels each, and up to five different types of non-fuel flow paths (i.e. bypasses). With the subchannel modelling approach the flow distribution in the core can be determined. Instead, for safety calculations the single channel approach is usually implemented, by considering the limiting (hottest) channel in the core.

2.2 Code NATCON

The code NATCON [4] has been written to analyze the steady-state thermal-hydraulics of plate-type fuel in a research reactor cooled by natural convection. The reactor core is immersed within a pool of water that is assumed to be at a constant temperature. The flow is determined iteratively from the balance between buoyancy and friction. The code computes coolant flow rate, axial temperature distributions (in both coolant and fuel) and the margin to ONB (Onset of Nucleate Boiling). Hot channel factors may be introduced for determining safety margins.

2.3 Code PARET

The code PARET has been originally developed at INEL (Idaho National Engineering Laboratory) and subsequently improved at ANL (Argonne National Laboratory) [5, 6]. It is a widely used calculational tool for carrying out coupled neutronic, thermal-hydraulic simulations in research reactors. The code employs one-dimensional hydrodynamics, one-dimensional heat transfer, and point kinetics with continuous reactivity feedback. A simplified void fraction model is included that estimates the voiding produced by subcooled boiling. The code has been validated against experimental results from power transient tests in small reactors (the SPERT experimental programme). The comparison with the experimental data was generally favourable. The obtained agreement was in the range between 10 to 40% in terms of power, released energy and clad temperature, over a wide range of initial reactor conditions.

The original version of the code assumes a constant core inlet temperature (or, equivalently, pool water temperature). The in-house version has been extended to accommodate pool heat-up, and thus provide a capability for analyzing very long transients in which significant pool temperature variations may be encountered (e.g. in the loss-of-secondary-cooling situations).

3 STEADY-STATE CALCULATIONS

The steady-state thermal-hydraulic behaviour of the LEU core is not expected to be significantly different from that of the HEU core, because in both configurations the core geometry, the power level and the flow rate remain the same. However, steady-state analyses have been performed with PARET and NATCON for benchmarking and testing purposes.

The calculations have been performed by considering a single hot channel and specifying appropriate engineering hot-channel factors. The latter are intended to account for fuel fabrication tolerances, uncertainties in calculated parameters, and uncertainties in the ability to measure certain variables such as the reactor power. The engineering hot-channel factors are applied as three separate components corresponding to: (i) uncertainties that affect the heat flux f_b , such that $Q_{hc}=Q_{nc}f_b$; (ii) uncertainties in the flow or enthalpy rise in the channel f_q , such that $m_{hc}=m_{nc}/f_q$, (iii) uncertainties in the heat transfer to the coolant f_h , such that $h_{hc}=h_{nc}/f_h$. In the previous notations hc refers to the hot channel and nc to the nominal channel values for the heat flux (Q), mass flow rate (m), and the heat transfer coefficient (h). The engineering hot-channel factors have been determined from uncertainties allowed in the LEU fuel element specifications and the SAR. The used engineering factors are summarized in Table I.

3.1 Calculation of safety limits in the forced convection mode

The safety limit in the forced convection mode is specified in terms of an operating envelope of limiting inlet temperatures as function of the flow rate, with the reactor operating at the power trip level of 6.5 MW and the coolant outlet temperature at its maximum permissible value of 56°C. This envelope has been determined with PLTEMP. The results are shown in Fig. 1. The original envelop specified for the HEU core is included for comparison. As can be seen, when the analysis does not include hot channel engineering peaking factors, the predicted values are in very close agreement with the original specifications for the HEU core. With peaking factors included in the analysis (see Table I), a lower envelop for the inlet temperature is predicted. However, the deviation from the original specifications is not large.

Sources of uncertainty	Uncertainties (%)		
	Heat flux	Enthalpy rise	Heat Transfer
Mass Loading	2	2	-
Meat Thickness	5	-	-
Channel Thickness	-	16	3
Fuel Homogeneity	20	5	-
Flow	-	10	8
Power	5	5	5
Heat Transfer Coeff.	-	-	20
Statistical Combination	$f_b=1.21$	$f_q=1.20$	$f_h=1.30$

Table I. Engineering hot-channel factors.

3.2 Calculation of safety limits in the natural convection mode

According to the specifications, the reactor power should not exceed 400 kW during operation in the natural convection mode. This limit was established as the half of a maximum theoretical value of 780 kW. The latter was found in early calculations [2] to be the power limit at which “cladding temperature shall not reach the boiling point of the water coolant”. Here, this limit is taken to mean the Onset of Nucleate Boiling (ONB) point rather than the bulk boiling point of the coolant.

The NATCON code was repeatedly run by increasing gradually the reactor power, until an indication of ONB is obtained in the hot channel, according to the correlation of Bergles-Rohsenow. The engineering hot-channel factors of Table I were used, whereas the reactor inlet temperature was taken to be at the limit value specified for the natural convection mode, namely 56°C. The maximum permissible power was determined to be 814 kW. Fig. 2 shows the clad and coolant temperatures as functions of core height, obtained at the maximum power conditions. As can be seen, nucleate boiling is effectively predicted in the upper half of the core, close to the core mid-plane. Note that the value of 814 kW compares well with the original power prediction of 780 kW.

4 TRANSIENT CALCULATIONS

In the present analysis, transient calculations have been performed for the two following types of reactor accidents

- (i) insertion of excess reactivity,
- (ii) loss of primary flow.

The above accidents have been selected on the basis of the suggestions on the initiating events, typically recommended for research reactors [9]. Moreover, cases (i) and (ii) above are precisely the cases considered in the IAEA benchmark exercise on reactor computational methods [10, 11].

Note that in the safety analysis performed for the original HEU core [2] no credit was given to the effects arising from the inherent feedback mechanisms (Doppler effects, voids, etc.). Most likely, this was due to the unavailability at that time of a coupled neutronics, thermal-hydraulics calculational tool. Eventually, this may be acceptable for a HEU core, characterized by weak feedback mechanisms [6, 12]. Instead, for the case of a LEU core reactor feedback has to be considered. The code PARET was found well suited for investigating such cases. The whole analysis is described next.

Λ (μs)	57.6
β_{eff}	0.0066
a_M ($\$/\text{g cm}^{-3}$)	35.799 (=0.35799 $\$/\%$ void)
a_T ($\$/\text{ }^\circ\text{C}$)	1.341×10^{-2}
a_F ($\$/\text{ }^\circ\text{C}$) LEU	2.37×10^{-3}
a_F ($\$/\text{ }^\circ\text{C}$) HEU	3.60×10^{-5}

Table II. Kinetic parameters and feedback coefficients. Λ is mean neutron generation time and β_{eff} is delayed neutron fraction. a_M , a_T and a_F are the reactivity coefficients due to changes of coolant density or void, coolant temperature (spectrum effects) and fuel temperature (Doppler effects), respectively.

4.1 Reactor Model

The reference configuration considered in the analysis is the equilibrium LEU core consisting of 33 elements (28 standard plus 5 control elements) with a Be reflector on two opposite faces. Axially, a chopped cosine power profile is assumed, having a peak value such that

$$(\text{peak power in the plate})/(\text{average power in the plate}) = 1.428.$$

On the other hand, the total peaking factor, defined as

$$F_p = (\text{maximum power in the core})/(\text{average power in the core}),$$

is taken equal to 2.1099. These values have been inferred from early reactor analyses performed for various GRR-1 configurations [13]. Note that the considered peaking factors are very close to the values of 1.5 (axial) and 2.1 (total), postulated for a typical pool-type research reactor in the IAEA benchmark exercise [10, 11].

The kinetic parameters and feedback coefficients used are summarized in Table II. The data have been inferred from the reactor calculations reported in [13]. The considered values are close to those typically employed in such type of reactor [6, 12]. Among the considered parameters, Doppler coefficient of reactivity is the only one that changes by orders of magnitude in the HEU to LEU transition. To cover the transition core configurations (mixed LEU/HEU), the calculations are performed with both values of the Doppler coefficient of reactivity. A separate parametric study ascertained that the sensitivity of the results to variations in the other kinetic parameters is less important.

In the simulations a two channel model was utilized in the PARET code. One channel represented the hottest flow channel and associated plate in the core, and the second represented the remainder of the core, i.e. average core conditions. Each channel contributes to the reactivity feedback through an externally specified weight coefficient. These coefficients have been determined in a simple volume-weight sense. The results reported are of the hottest channel only.

4.2 Simulation of maximum start-up accident

A maximum start-up accident is considered, by assuming that the five control rods are all withdrawn in a continuous mode at their constant speed. From the linear part of the reactivity versus distance curve of the control rods we get a total rate of reactivity insertion of $R = 5.43 \cdot 10^{-4} \delta k / k / \text{sec}$. The period trips are assumed to fail, and the trip is taken on the maximum power limit of $N = 6.5$ MW (130% of full power). The corresponding minimum period at

the trip level is $T = \left(\frac{\Lambda}{2R \ln\left(\frac{N}{N_0}\right)} \right)^{1/2}$ where N_0 is the initial power level (of the order of 10^{-1} W),

depending on the source strength and the subcritical multiplication factor. The minimum period is estimated to be 56.3 ms. From the inhour equation it is found that the above period corresponds to an excess reactivity of $\rho_0 = 7.84 \cdot 10^{-3} \delta k / k$, or 1.19 \$. In the calculations, the insertion of reactivity is idealized by a step function. A separate case without scram is also considered.

The time variation of reactor power is shown in Fig. 3a. As can be seen, the power excursion may terminate even without action of the control rods (case without scram), although at a much higher peak value. This is a demonstration of the strong feedback mechanisms. As expected, the feedback is stronger with LEU fuel because of enhanced Doppler effects. The effect is marked in the case without scram, whereas in the case with scram the effect is negligible. The time variation of the clad temperature is shown in Fig. 3b. In both cases with and without scram, the peak clad temperature remains well below the melting point of aluminium which is about 600°C. Hence, the considered maximum start-up accident does not have any safety implication for the core.

4.3 Simulation of maximum reactivity insertion accident

The case of the maximum reactivity insertion accident is considered. The assumed event consists of a step reactivity insertion of $\rho_0 = 0.02 \delta k / k$ while the reactor is operating at 5 MW. This amount of reactivity corresponds to a sudden addition of an extra fuel element in the matrix, assumed to have dropped inadvertently during a crane manipulation. Note that the probability of such an event is extremely low because according to the regulations no crane manipulation is permitted when the reactor is at full power. However the analysis of this reactivity accident is instructive because it envelops all other conceivable reactivity accidents, such as start-up accidents, loading accidents, influences from experimental facilities etc.

The postulated accident corresponds to a large reactivity insertion of 3.04 \$. Since the reactivity is considerably larger than 1 \$, the power excursion is dominated by the prompt period

$T = \frac{\Lambda}{\rho_0 - \beta_{\text{eff}}}$ which in the present case is equal to 4.3 ms. In the analysis we assume that the period trips fail, and that reactor scrams on the over-power trip, triggered at 130% of the nominal full power. Rod drop is assumed to initiate 5 ms after power exceeds 6.5 MW. This is the fast scram case, caused by cutoff of the magnet currents, as opposed to the slow scram case (delay of 20 ms), caused by opening the power circuit of the magnet power supply. The acceleration of rod drop is pessimistically taken as half of the acceleration due to gravity. As previously, the case without scram is also considered, for both HEU and LEU fuels.

The evolution of power is shown in Fig. 4a. Reactor power rises very rapidly, and the trip level of 6.5 MW is attained at about 4 ms. However, due to the rod drop delay time, the power continues to rise well above the trip level, and reaches a peak point at 30 ms. In the simulation with the reactor scram "on", a power peak of 940 MW is obtained for the LEU fuel. As before, with HEU fuel more adverse conditions are obtained during the transient, because of the weaker feedback (power peak of 1100 MW). With the scram disabled the obtained values are significantly higher (above 2000 MW).

The clad temperature profiles are plotted in Fig. 4b. With the scram enabled, the maximum point is obtained at 53 ms and corresponds to clad temperatures of 410°C and 475°C for the LEU and HEU cases, respectively. Still, however, these values are below the safety limit of 600°C. Instead, if the reactor protection system fails, the clad temperature exceeds the clad melting point 40 ms following accident initiation. Thus, in this case, core damage occurs.

4.4 Simulation of maximum loss-of-flow accident

The simulation of loss-of-flow transients has been the object of a detailed investigation [14], motivated by the fact that very limited literature exists on the subject, as opposed to the abundant literature existing on reactivity transients. The full analysis can be found in [14]. Next, an extended summary is given.

It is assumed that the reactor cooling system is operating at its nominal flow rate of 450 m³/h when a 100% loss-of-flow occurs. The flow rate decay is approximated by an exponential function as

$$G = G_0 \exp(-t/\tau) \quad (1)$$

where G_0 is the initial flow rate and τ a time constant describing the rapidity of the decay. The time constant τ is either 1 s corresponding to a fast transient (e.g. valve failure) or 25 s corresponding to a slow transient (e.g. pump failure with large flow inertia).

Provision is made to account for pool heating, considering that after a loss-of-flow event reactor power cannot be discharged to the heat exchanger. The original version of PARET assumes a constant core inlet temperature. A customized version of the code was devised, in which core inlet temperature is determined from a stationary heat balance over the pool volume. Accordingly, core inlet temperature is prescribed to vary as

$$T_{\text{inlet}} = T_0 + \frac{\int_0^t V_{\text{fuel}} P(t') dt'}{\rho_c c_{pc} V_{\text{pool}}} \quad (2)$$

where $\rho_c c_{pc}$ is the volumetric heat capacity of the coolant (water), V_{fuel} the fuel volume, and V_{pool} the volume of the pool. At $t = 2\tau$, i.e. when flow-rate G reduces to $\approx 15\%$ of the initial value G_0 , the flapper valve sealing the lower plenum is assumed to open, hence, downward forced flow stops and natural circulation develops through flow reversal. This is the most adverse part of the transient because the hot coolant of the lower plenum will first undertake natural cooling, until cool water from the pool expels progressively the hot lower plenum volume. This phase is simulated as follows: inlet coolant temperature T_{inlet} is forced to jump to the value of the exit coolant temperature predicted at $t = 2\tau$, and then is forced to match again Eq. (2). In flow reversal conditions, low-pressure systems like research reactors are susceptible to a form of instability known as flow excursion or Ledinegg instability [17, 18]. This instability, which is due to a negative slope in the pressure drop versus flow-rate curve, can be described as follows. In the occurrence of massive vapour generation, liquid phase is forced to accelerate to compensate for the large flow area reduction (gas-to-liquid specific volume ratio is very high at low pressure). This creates a significant pressure drop, thereby lowering flow-rate through the channel, which in turn leads to more vapour generation. As a result, clad surface may experience premature burnout, as indeed has been observed in experimental investigations [16]. Instead, if the transient is free of instabilities, then one may reasonably anticipate that the accident, even unprotected, will be self-terminated due to reactor feedback, without compromising core integrity. Based on this remark, the analysis focuses on determining the stability boundaries and their sensitivity to relevant operational and physical parameters. The threshold conditions for flow instability are determined using the developments of Whittle and Forgan [16]. The latter proposed a correlation for the Onset of Flow Instability (OFI) point in terms of a critical value for the ratio

$$R = \frac{T_{\text{out}} - T_{\text{inlet}}}{T_{\text{sat}} - T_{\text{inlet}}} \quad (3)$$

as follows

$$R_{\text{OFI}} = \frac{1}{1 + 25 \frac{D_e}{H}} \quad (4)$$

where H is the height of the channel, D_e the equivalent hydraulic diameter and T_{out} and T_{sat} are the outlet and saturation temperatures respectively. The above correlation has been inferred from measurements in narrow rectangular channels at low-pressure conditions and proved to be the most satisfactory for research reactor applications [11, 17, 19].

The simulations were done with and without scram. In the simulations with scram, the trip setting is at the low flow limit of 160 m³/h (36% of the nominal value). Also, a time delay of 20 ms was inserted before the shutdown reactivity insertion initiates (slow scram assumed). In all these cases, the peak clad temperatures computed during the transient were of the order of 90°C, thus, far below the melting temperature of the cladding. Hence, the cases with scram do not raise any safety issue. The same conclusion was obtained in previous calculations performed with PARET [15].

The results of the simulations without scram depend predominantly on the initial power level and initial pool temperature. With reduced initial power and initial pool temperature, no significant bulk boiling takes place during flow reversal, and stable natural cooling conditions are ultimately established. Instead, starting with elevated initial power or pool temperature, vigorous boiling is predicted, inducing flow instabilities. Figure 5a illustrates the response of clad temperature for three typical cases, namely, with scram (case 1), without scram and stable conditions (case 2), and without scram and unstable conditions (case 3). Clearly, as stated before, case 1 does not imply any consequence. In case 2, although the clad temperature response exhibits a sharp peak, it remains well below the safety limit of 600°C. In case 3, clad temperature exceeds the ONB point, vigorous boiling initiates and the system is ultimately found under unstable conditions (OFI point encountered). The course of the transient is not further predicted. An accurate description of the unstable part of the transient would require a full two-phase modelling approach, with an accurate calculation of stagnant conditions. PARET code is limited in this respect, for it employs incompressible hydrodynamics and simplified void generation equations.

The power profile is shown in Fig. 5b. Obviously, in the shut-down case (case 1), the reactor power drops immediately to the decay power level. In the case without scram but stable conditions (case 2) the reactor power reduces constantly due to feedback, and is found stabilized at the end of the transient at the level of 340 kW. One may thus conclude that at longer periods the core still remains under safe conditions. Indeed, a simple energy balance shows that at such power levels, continuous heating of approximately 56 h is required prior to reaching bulk boiling conditions in the reactor pool.

Figure 6 shows the calculated boundary between region A, where the whole transient remains stable (i.e. no OFI point is encountered during the simulation), and region B, where the system goes into an unstable regime. The envelope is shown in terms of maximum tolerable pool temperature as function of the initial reactor power. Two envelopes are shown, corresponding respectively to the conditions of a slow transient (decay flow rate period of $\tau = 25$ s) and a fast transient ($\tau = 1$ s). A separate sensitivity analysis ascertained that period τ is the most important influencing parameter. Instead, the kinetic parameters, (mean neutron generation time Λ and delayed neutron fraction β_{eff}) were found to exert negligible influence on the output results. The reactivity coefficients have a measurable effect on the results, yet, their impact is rather restrained and would not alter significantly the results of Fig. 6. An exception to that is the case of the Doppler coefficient. Markedly wider stability margins are obtained with LEU, as indicated by the vertical bar shown in Fig. 6. This finding is another demonstration of the safety enhancement achieved with the use of LEU fuel in research reactors.

The horizontal dashed line of Fig. 6 shows the maximum pool temperature which may be expected during reactor operation, whereas the vertical dashed line shows the maximum power level. In this way, the safe and unsafe regions of initial conditions are fully delineated. As can be seen, with a slow transient, an unprotected loss-of-flow event does not imply any consequence for the core if

initial pool temperature is below 38°C. Instead, in case of a very rapid loss-of-flow accident the core will experience flow instabilities, no matter what are the initial conditions.

4.5 Simulation of partial loss-of-flow accident

The case is concerned with the loss of 1 of the 2 primary pumps and simultaneous loss of secondary cooling. Such a sequence may arise, for instance, in a loss of off-site power event (the emergency unit provides power only for one primary pump). We assume an initial power of 5 MW and a maximum initial pool temperature of 44°C. All safety trips are assumed to fail, hence, the reactor is not let to scram.

The core exit, clad, and pool water temperatures are shown in Fig. 7a, whereas the power variation with time is plotted in Fig. 7b. The 50% flow reduction gives rise to an initial overshoot of both clad and coolant temperatures prior to the establishment of the reduced-flow cooling conditions. The peak temperatures obtained are far below any safety concern. The temperature spikes induce quite strong feedback mechanisms, and as a result the power drops sharply at the beginning of the transient. Note that pool temperature increases gently, because secondary cooling is not available. This constant temperature rise introduces negative reactivity, causing a gradual power decrease at later times, as can be observed in Fig. 7b. After 7200 s (2 h) safe temperature and power levels are prevailing in the core. Rough estimations indicate that a further time period of 44 h is required prior to onset of boiling in the reactor pool. Hence there are comfortable time margins to undertake remedy actions.

5 ANALYSIS OF LOSS-OF-COOLANT ACCIDENT

The case of the most severe Loss-Of-Coolant Accident (LOCA), leading to a complete uncover of the core, is considered. In the Safety Report for the original HEU core [2] the LOCA accident has been analysed by calculating with THEAP code [1] reactor cooling through natural convection to air and radiation-conduction to the surrounding structures. This approach will not be pursued in the present analysis. Modelling of radiative and convective heat transfer to air in uncover core conditions is a complex problem with large uncertainties and with missing experimental data to qualify the predictions [7, 8]. Instead, the analysis is limited to a simplified (and pessimistic) heat transfer calculation considering a single channel and the associated fuel plates. Conductive or radiative heat losses are ignored and only convective heat transfer to air is allowed. The objective is to predict peak fuel plate temperatures in order to determine if the fuel melting point of 600°C will be reached.

We assume that the reactor is operating at full rated power (5 MW) and is shutdown when loss of coolant is detected (scrammed by the switch of the pool level sensor). The drain time is minimized by assuming that the failure occurs at the largest pipe at the bottom of the pool, i.e. at the 10-inch diameter inlet water pipe. As the water is draining from the pool it is further assumed that all of the reactor decay heat will be removed by natural circulation, up to the time the core fuel elements start becoming uncovered by the pool water. The term “lag time” is used to refer to this time difference between reactor shutdown and uncovering of the core fuel elements. The time point at which uncovering begins is considered to be the start of air cooling, i.e. $t = 0$ in the model discussed in Section 5.2. below.

5.1 Calculation of pool draining

The analysis is based on steady state fluid mechanics, considering that pool draining is a relatively slow transient. The starting point is the well-known Bernoulli equation that, with reference to Fig. 8, is written as

$$\rho gh - 2f \frac{l + l_{eq}}{D} \rho u^2 = \frac{1}{2} \rho u^2 \quad (5)$$

where l_{eq} is the equivalent length corresponding to exit pressure losses, ρ the water density, u the water exit velocity, g the acceleration due to gravity, and f the friction factor. The latter is taken as constant, by assuming fully turbulent regime. By differentiating with respect to time t , Eq. (5) gives

$$\frac{dh}{dt} = \frac{1 + 4fL/D}{g} u \frac{du}{dt} \quad (6)$$

where $L = l + l_{eq}$. On the other hand, from a simple mass balance one may write

$$\frac{dh}{dt} = -\frac{A_u}{A_g} u \quad (7)$$

where A_u and A_g are the areas of the horizontal cross-sections of the aperture and the pool, respectively (see Fig. 8). Although the system of differential equations (6) and (7) is nonlinear, its analytical integration can be easily undertaken. After some straightforward algebra, the following result is obtained

$$h = (h)_{t=0} - \frac{A_u}{A_g} \left(\frac{2gh_0}{1 + 4fL/D} \right)^{1/2} t + \frac{1}{2} \left(\frac{A_u}{A_g} \right)^2 \frac{g}{1 + 4fL/D} t^2 \quad (8)$$

The time evolution of the pool water height is plotted in Fig. 9 for $D = 10$ inch. As can be seen, core uncover will initiate after approximately 16 min ($t_{lg} = 16$ min), whereas the water pool will be completely emptied after 23 min.

5.2 Calculation of natural convection in air

5.2.1 Fission product decay heat

The decay heat is maximized by assuming an infinite reactor operating time prior to shutdown. The ratio P/P_0 where P is the decay power and P_0 the initial reactor power is determined with the help of the following relation, as available in [20]

$$\frac{P}{P_0} = C_F \cdot 0.095(t + t_{lg})^{-0.26} \quad (9)$$

where t is the time -in seconds- into air cooling (i.e. following core uncovering), t_{lg} the time lag (i.e. the period elapsed from reactor shutdown), and $C_F = 1.2$. The latter is a safety factor, suggested by the American Nuclear Society standard ANS-5.1/N18.6 to be used in the fission-product decay heat calculation in uranium-fuelled thermal reactors.

5.2.2 Physical model

A single channel system, as shown in Fig. 10 is considered. No conductive or radiative heat transfer is allowed in the model analysis. Convective heat loss is constrained by the width of the coolant channel within the fuel element. Therefore, convection is allowed to occur only from inside the channel and not from plate edges, which are taken as adiabatic surfaces.

Heat transfer is determined from the solution of the energy conservation equation, as formulated for a lumped heat capacity approach for the fuel plates and the associated cooling channel

$$\rho_f c_f d \frac{dT_f}{dt} = -h_T (T_f - T_c) + \frac{P}{2NS_f} \quad (10)$$

$$\rho_c c_c b \frac{dT_c}{dt} + \frac{2}{H} \rho_c c_c b U (T_c - T_\infty) = h_T (T_c - T_f) \quad (11)$$

where T is the temperature, ρ the density, c the specific heat, h_T the heat transfer coefficient, d the fuel plate half-width, b the cooling channel half-width, H the height of channel, S_f the fuel plate surface, U the air velocity in the channel, and N the number of plates in the core. The subscripts f , c , and ∞ refer to fuel plate, coolant (air) and free stream (ambient air), respectively.

For simplicity, the heat transfer coefficient is taken constant, determined as $h_T = \text{Nu} \lambda_c / D_H$, where λ_c is the air thermal conductivity, D_H the cooling channel hydraulic diameter, and Nu the Nusselt number. We used a Nusselt number $\text{Nu} = 7.5$. This selection is based on available analytical solutions for laminar-flow heat transfer in rectangular ducts of arbitrary aspect ratio.

The velocity U at which air rises in the channel is unknown, and has to be determined from the balance between buoyancy and frictional forces. The pressure differential due to buoyancy is

$$\Delta P = (\rho_\infty - \rho_c) g H \quad (12)$$

which, assuming ideal gas law becomes

$$\Delta P = \rho_c (T_c - T_\infty) g H / T_\infty \quad (13)$$

For simplicity, transient effects will be ignored, hence, the momentum balance can be expressed as

$$\frac{1}{2} \rho_c U^2 \left(1 + \sum \xi + 4f \frac{H}{D_H} \right) = \Delta P \quad (14)$$

where $\sum \xi$ the sum of the various local resistances such as inlet and exit effects, and f the friction factor. Assuming laminar flow, the friction factor is determined as $f = C_f / \text{Re}$ where C_f is a constant depending on the aspect ratio of the rectangular channel cross-section ($C_f = 96$ in the present case), and Re is the Reynolds number. The latter is defined by $\text{Re} = \rho_c U D_H / \mu_c$ where μ_c is air viscosity. By substituting the preceding expressions into Eq. (14), it can be easily verified that velocity U becomes the solution of a quadratic equation. The result is

$$U = \frac{-4C_f \mu_c H / \rho_c D_H^2 + \sqrt{\Delta}}{2(1 + \sum \xi)} \quad (15)$$

where the discriminant Δ is

$$\Delta = \left(4C_f \mu_c H / \rho_c D_H^2\right)^2 + 8\left(1 + \sum \xi\right) \Delta P / \rho_c \quad (16)$$

Equations (9)-(11), in conjunction with Eqs. (13), (15) and (16) give rise to a nonlinear dynamic system that can be solved numerically. The numerical solution was obtained with a purposely-developed *Matlab* program that employed *Simulink* and the built-in solvers for Ordinary Differential Equations (ODEs). Numerical trials with Eqs. (13), (15) and (16) permitted to ascertain that within the ranges of interest the air velocity U is, to a very good approximation, a simple linear function of the temperature difference $T_c - T_\infty$, namely

$$U = K(T_c - T_\infty) \quad (17)$$

where the proportionality constant K can be easily determined in every case from a numerical experiment. Although Eq. (17) does not remove the nonlinearity from the system, its use in place of the exact formulae, improved spectacularly the convergence characteristics of the numerical solution.

5.3 Results

The time evolution of the fuel plate temperature is shown in Fig. 11, for various time lag periods. In all these calculations, the ambient air temperature in the reactor hall (which is an air-conditioned room) was pessimistically taken as $T_\infty = 308$ K (35°C). As can be seen, for the severest case addressed in section 5.1. ($t_{lg} = 16$ min), fuel melting is effectively predicted after about 2 h 15 min, following core uncover (i.e. 2 h 30 min after the initiating event). Also, the results of Fig. 11 indicate that a lag period of 1.5 h is at least required to avoid core melting. For longer time lags, air natural convection is seen to be adequate to remove decay-heat generation.

6 CONCLUSIONS

The Research Reactor Laboratory has been equipped with appropriate calculational capabilities, as needed for performing safety assessments in house. The available codes are PLTEMP, NATCON and PARET. The codes have been installed on a PC, and are all currently operational.

The codes have been used to assess the safety issues of the core conversion from Highly Enriched Uranium (HEU) fuel to Low Enriched Uranium (LEU) fuel. A simplified heat transfer model has been also developed to calculate core temperature in case of a core uncover (loss-of-coolant accident).

It was found that:

1. The safety limits in steady-state operation, as specified in the safety report for the original HEU core, remain practically the same for the LEU core, both for the forced convection mode and the natural convection mode.
2. The maximum start-up accident does not lead to core damage, regardless of the availability of the reactor protection system (i.e. both with and without automatic reactor shut-down).
3. The maximum reactivity accident does not lead to core damage, provided that a fast scram is successfully triggered. Instead, with the reactor unprotected, clad melting will take place.
4. A total loss-of-flow event followed by reactor shut-down does not raise any safety issue. With the reactor unprotected, the course of the transient depends predominantly on the following parameters: initial pool water temperature, initial power, and flow rate decay period. A chart has been derived, specifying the regions of safe and unsafe initial conditions.

5. A 50% loss-of-flow event (failure of 1 pump), does not have any safety implication, even under the pessimistic assumptions of automatic shut-down failure and loss of secondary cooling.
6. The maximum loss-of-coolant event (complete break of the 10-inch inlet pipe) will lead to core uncover after 16 min and complete pool drainage after 23 min. Air cooling is not adequate to remove decay heat (hence, core melt will occur), unless more than 1½ h have elapsed since reactor shutdown.

In general, safety is promoted with the use of LEU fuel in the core. This is mainly attributed to the Doppler effect, which is significant in the LEU fuel because of the abundance of the contained U-238. In all the above transient simulations, strong feedback responses were predicted, contributing significantly to inherent reactor power drop

7 REFERENCES

1. Bartzis, J. G., Megaritou, A., and Belessiotis, V. (1987) *THEAP-I. A Computer Program for Thermal Hydraulic Analysis of a Thermally Interacting Channel Bundle of Complex Geometry. Code Description and User's Manual*. National Centre for Scientific Research Demokritos, Report DEMO 87/10.
2. Papastergiou, C. (Ed.) (1985), *Safety Analysis Report of the Greek Research Reactor-1 (GRR-1)*. National Centre for Scientific Research Demokritos, Institute of Nuclear Technology and Radiation Protection.
3. Mishima, K., Kanda, K., and Shibata, T. (1984) *Thermal-Hydraulic Analysis for Core Conversion to the Use of Low-Enriched Uranium Fuels in the KUR*. Research Reactor Institute, Kyoto University, Report KURRI-TR-258.
4. Smith, R. S., and Woodruff, W. L. (1987) *Thermal-Hydraulic Analysis and Safety Margins for Natural Convection Cooled Research Reactors*. Argonne National Laboratory, Report ANL/PERTR/TM-12.
5. Obenchain, C. F. (1969) *PARET-A Program for the Analysis of Reactor Transients*. Idaho National Engineering Laboratory, Report IDO-17282.
6. Woodruff, W. L. (1984), A kinetics and thermal-hydraulics capability for the analysis of research reactors, *Nuclear Technology* **64**, 196-206.
7. Woodruff, W. L. (1998), Personal Communication.
8. Argonne National Laboratory (1981) *U. S. Contributions to IAEA Guidebook on the Safety and Licensing Aspects of Research Reactor Core Conversions from HEU to LEU fuels*. Report ANL-229 (2-75), March 1981.
9. IAEA (1994) *Safety Assessment of Research Reactors and Preparation of the Safety Analysis Report*. International Atomic Energy Agency, Report IAEA-SAFETY SERIES No 35-G1.
10. IAEA (1992) *Research Reactor Core Conversion Guidebook*. International Atomic Energy Agency, Report IAEA-TECDOC-643.
11. IAEA (1980) *Research Reactor Core Conversion from Use of Highly Enriched Uranium to the Use of Low Enriched Uranium Fuels Guidebook*. International Atomic Energy Agency, Report IAEA-TECDOC-233.
12. Mirza, A. M., Khanam, S., and Mirza, N. M. (1998), Simulation of reactivity transients in current MTRs, *Annals of Nuclear Energy* **25**, 1465-1484.

13. Papastergiou, C. and Deen, J. R., (1981) *Neutronic Calculations for the Conversion of the GRR-1 Reactor from HEU Fuel to LEU Fuel*, Argonne National Laboratory, Unpublished Report ANL, November 1981.
14. Housiadas, C. (2000), Simulation of loss-of-flow transients in research reactors, *Annals of Nuclear Energy* **27**, 1683-1693.
15. Woodruff, W. L., Deen, J. R., and Papastergiou, C. (1994), *Transient Analyses and Thermal-hydraulic Safety Margins for the Greek Research Reactor (GRR1)*, Proceedings of the International Meeting on Reduced Enrichment for Research and Test Reactors, Williamsburg, Virginia, 18-23 September 1994, Argonne National Laboratory, Report ANL/RERTR/TM-20 CONF-9409107.
16. Whittle, R. H. and Forgan, R. (1967), A correlation for the minima in the pressure drop versus flow rate curves for subcooled water flowing in narrow heated channel, *Nuclear Engineering and Design* **6**, 89-99.
17. Hu, L. W. and Bernard, J. A. (1999), Thermal-hydraulic criteria for the MIT research reactor safety limits calculation, *Transactions of the American Nuclear Society* **81**, 114-115.
18. Oh, C. H. and Chapman, J. C. (1996), Two-phase flow instability for low-flow boiling in vertical uniformly heated thin rectangular channels, *Nuclear Technology* **113**, 327-337.
19. Mishima, K., Kanda, K. and Shibata, T. (1984), *Thermal-hydraulic analysis for core conversion to the use of low-enriched uranium fuels in the KUR research reactor*, Kyoto University, Report KURRI-TR-258.
20. El-Wakil, M. M. (1971), *Nuclear Heat Transport*, International Textbook Company, New-York.

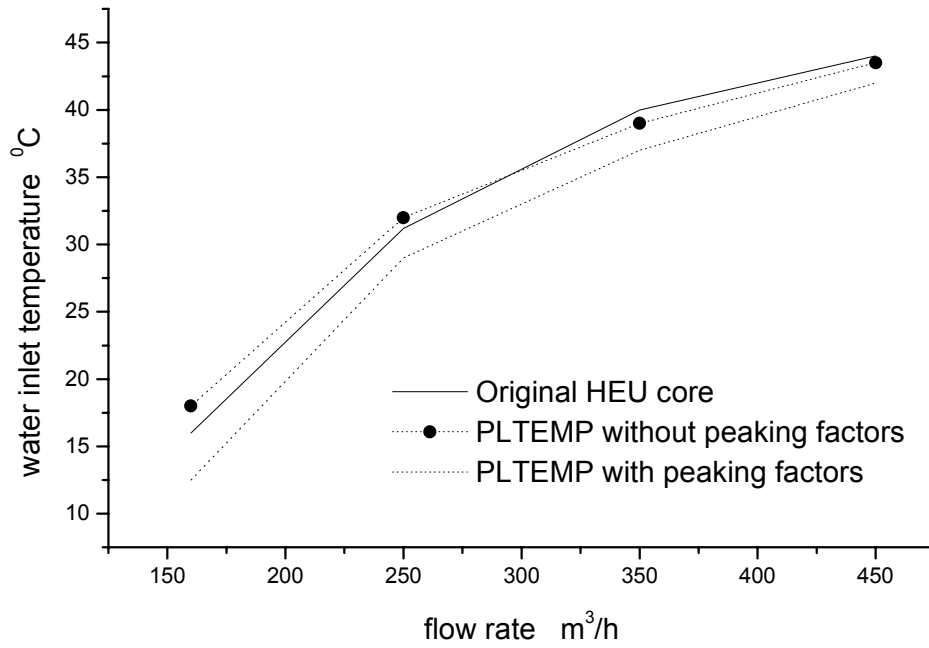


Fig. 1. Limit core inlet temperature as function of flow rate in the forced convection mode.

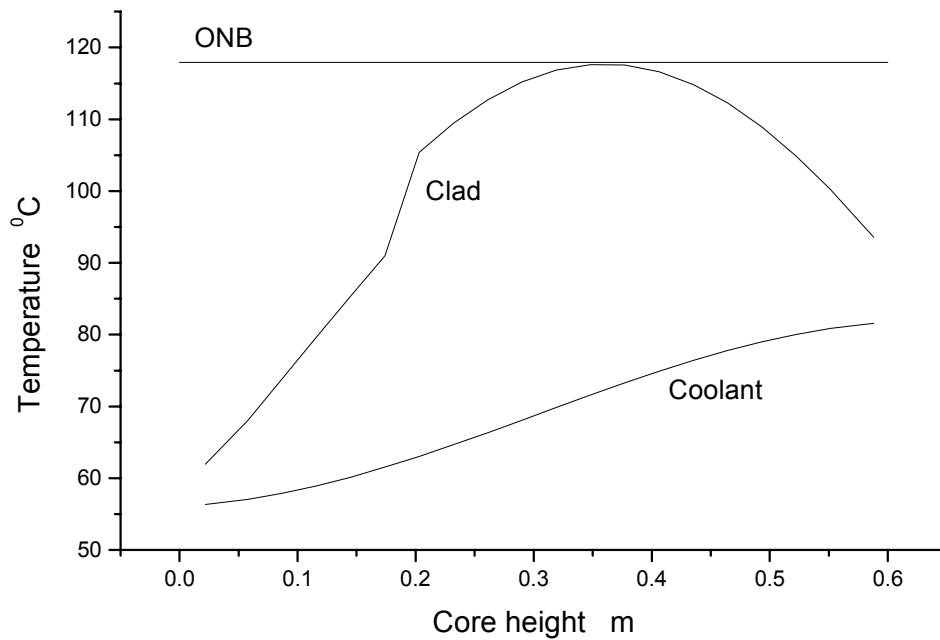


Fig. 2. Axial distribution of clad and coolant temperatures in the natural convection mode at the maximum power of 814 kW.

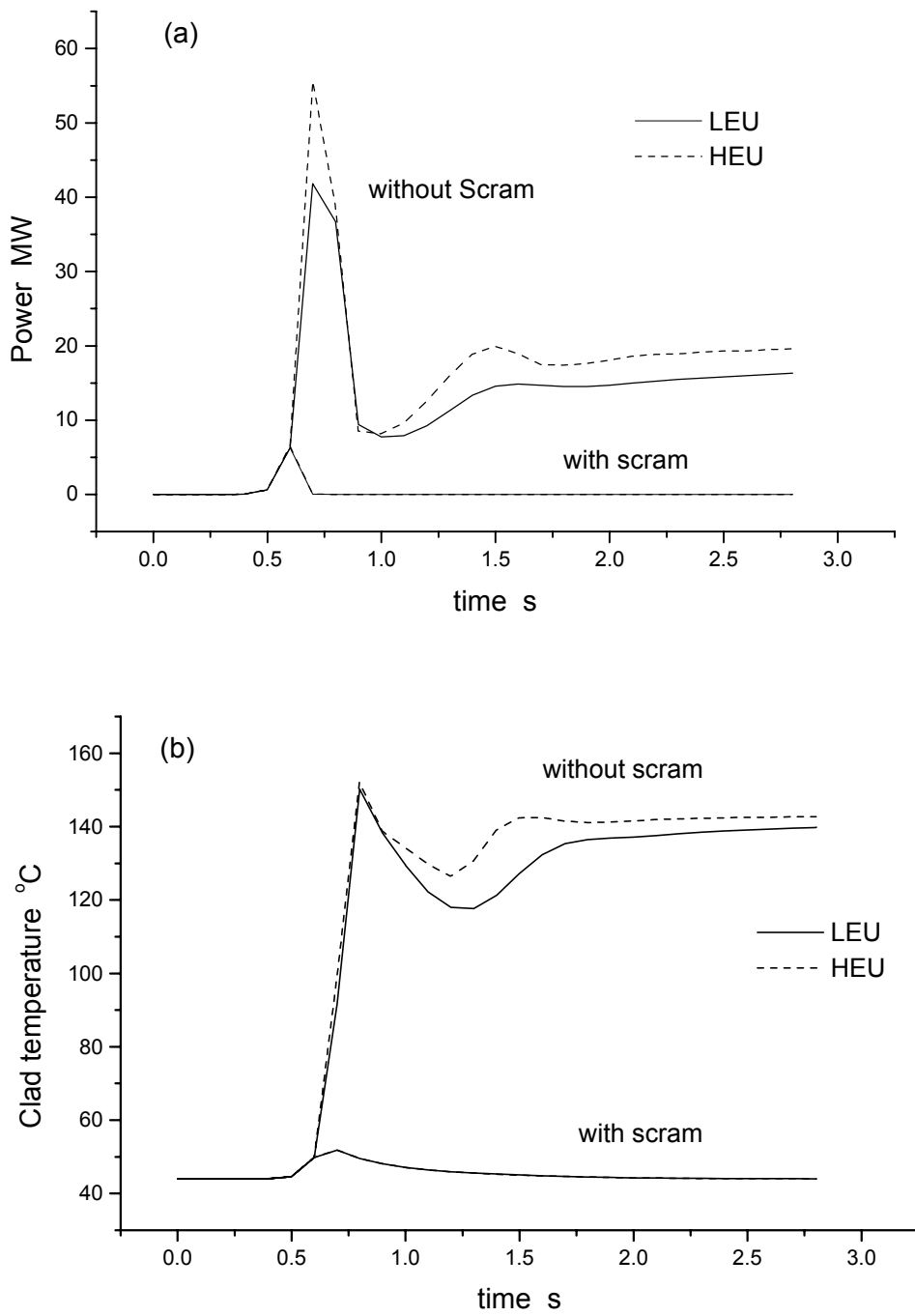


Fig. 3. Maximum start-up accident. Time variation of power (a) and clad temperature (b).

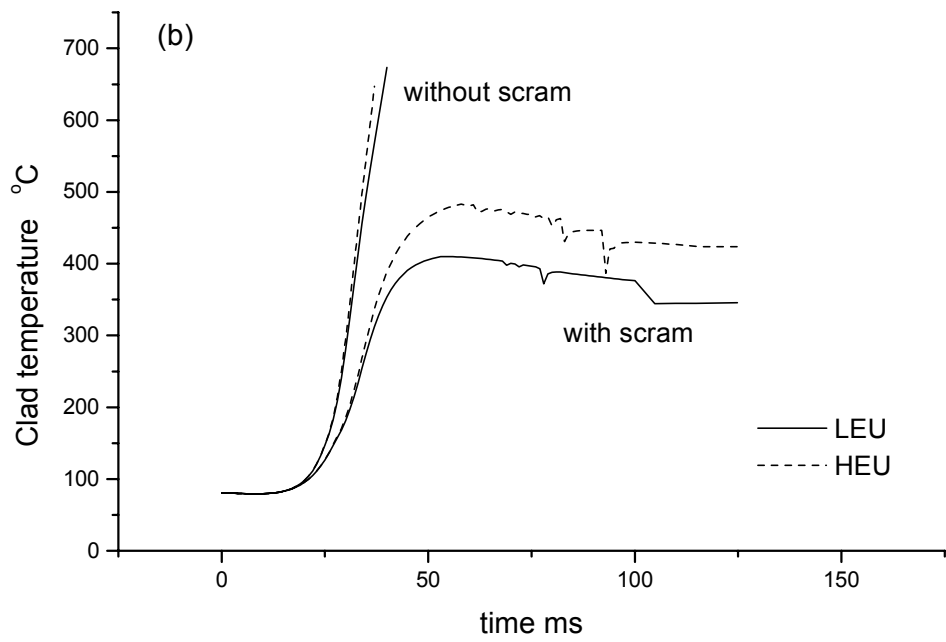
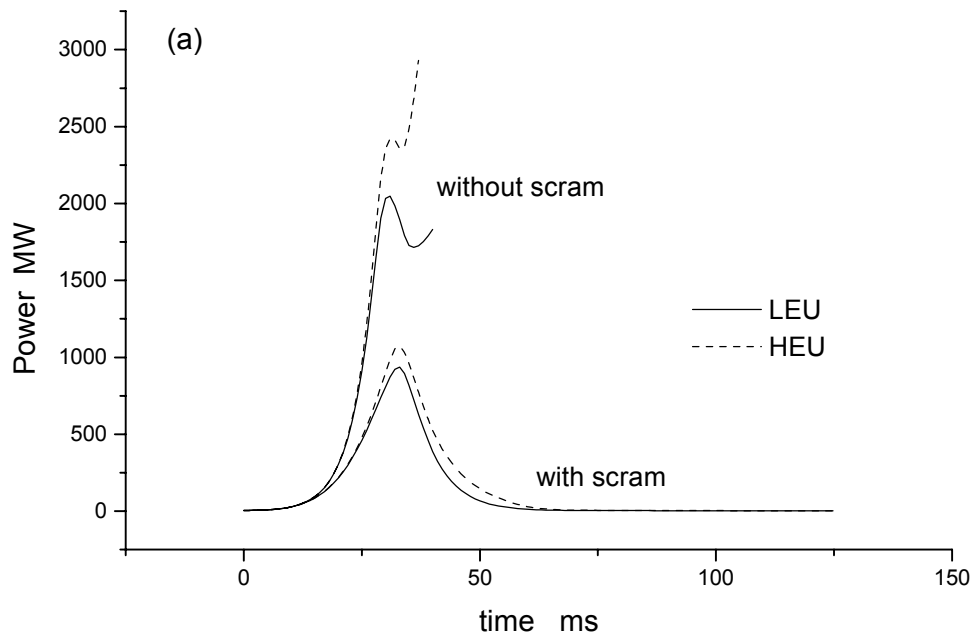


Fig. 4. Maximum reactivity accident. Time variation of power (a) and clad temperature (b).

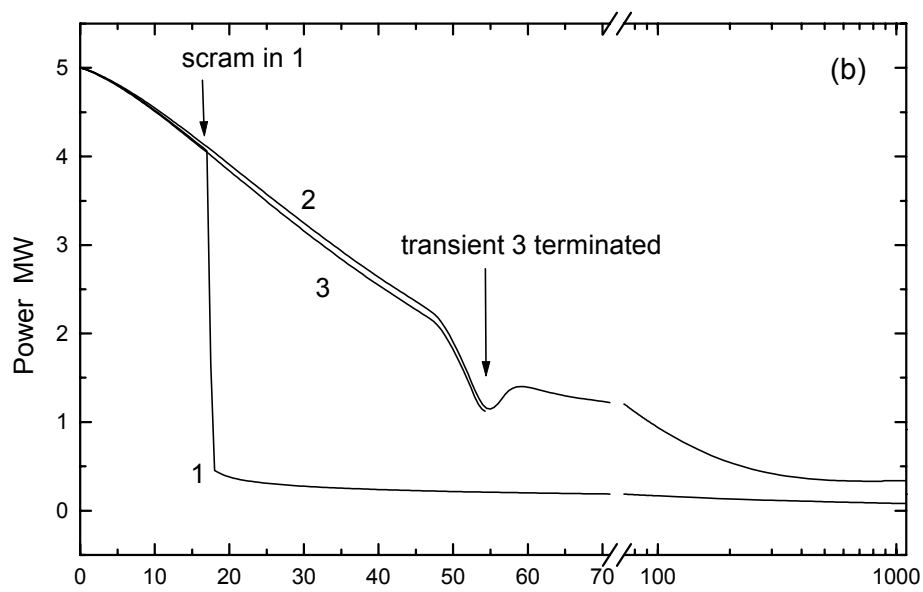
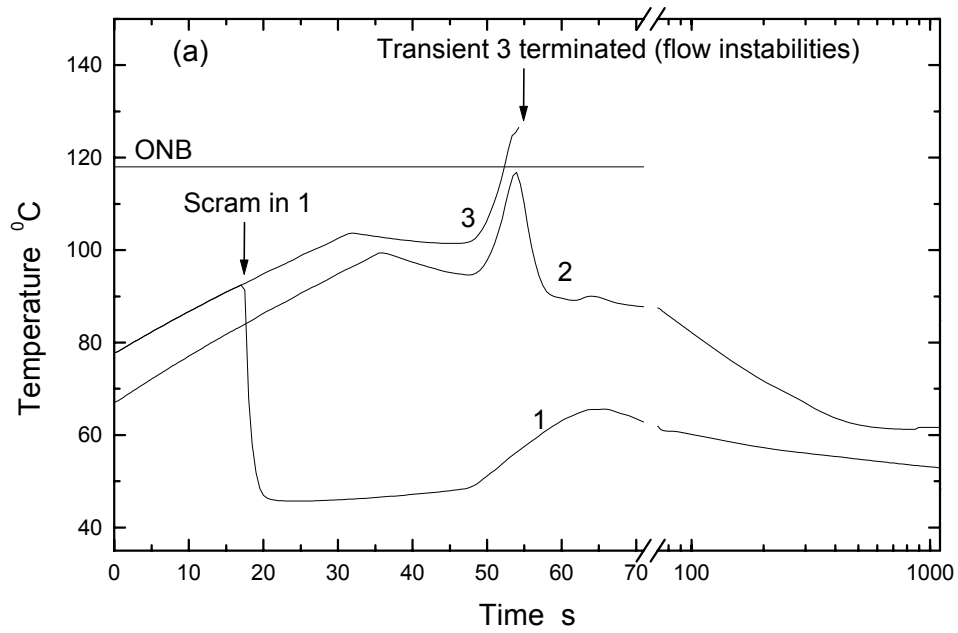


Fig. 5. Loss-of-flow transient. Responses of clad temperature (a) and power (b). Initial power $P_0=5$ MW, initial pool temperature $T_0=40^\circ\text{C}$ (cases 1 and 3), or $T_0=25^\circ\text{C}$ (case 2). Flow decay parameter $\tau=25$ s.

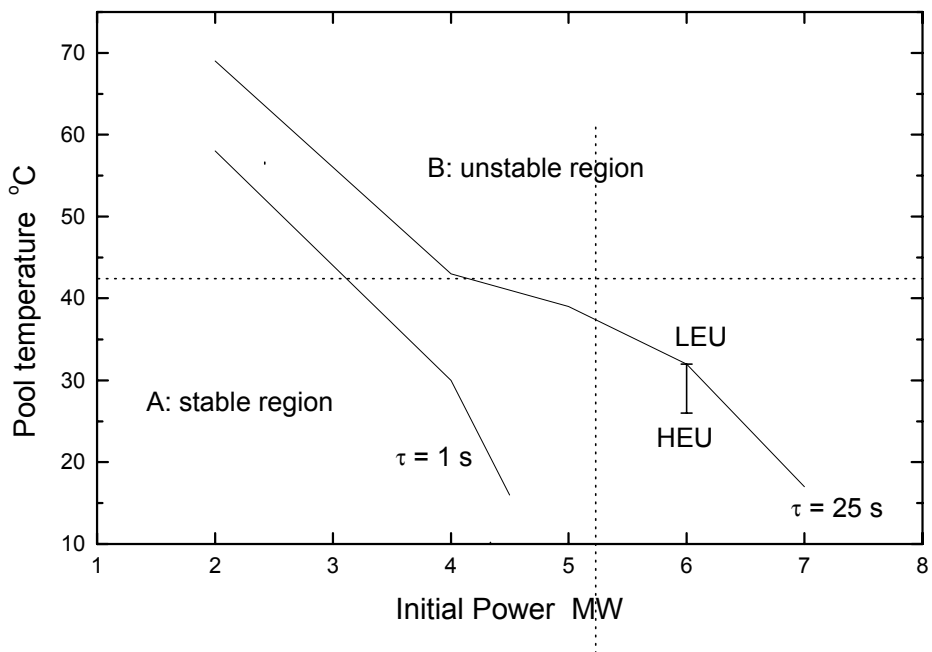


Fig. 6. Maximum pool temperature as function of initial power for stable loss-of-flow transient without scram.

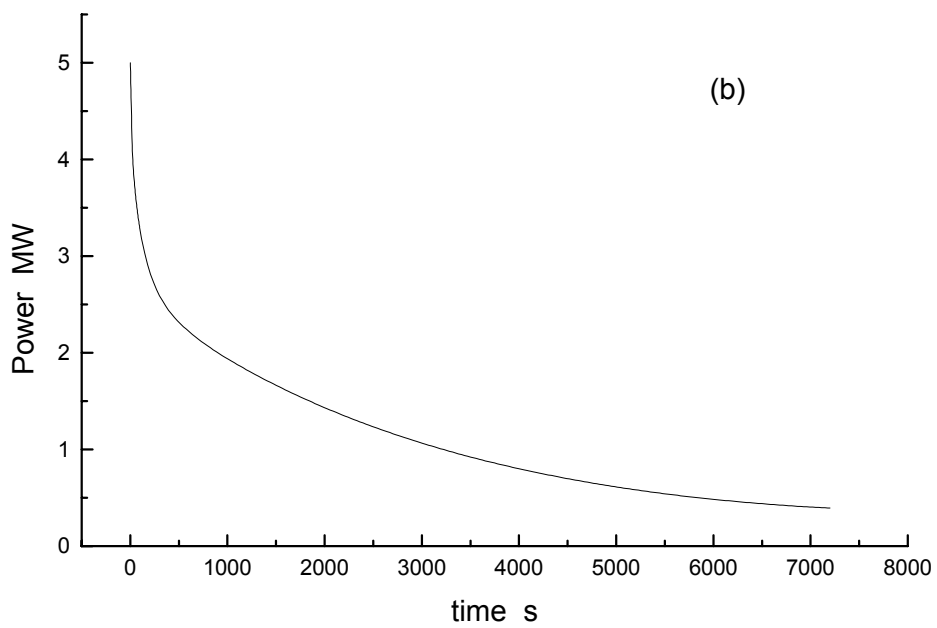
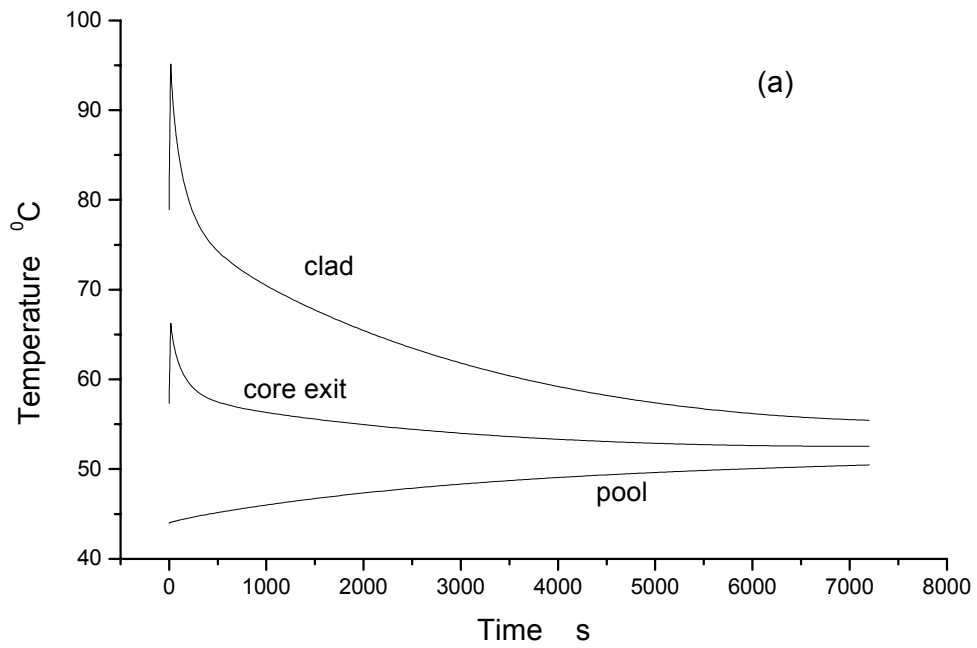


Fig. 7. Partial loss-of-flow-transient. Responses of clad, core exit, and pool temperatures (a), and reactor power (b).

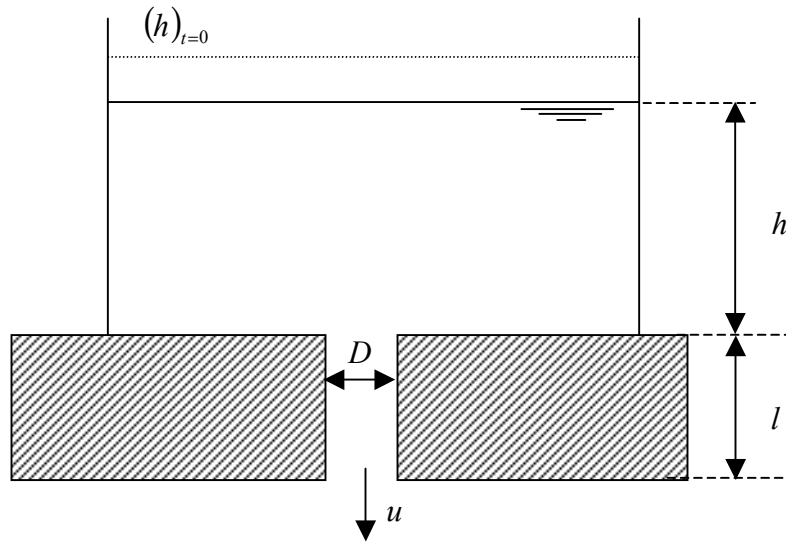


Fig. 8. Schematic of pool draining through an aperture at the bottom of diameter D . l is the thickness of the concrete walls surrounding the pool.

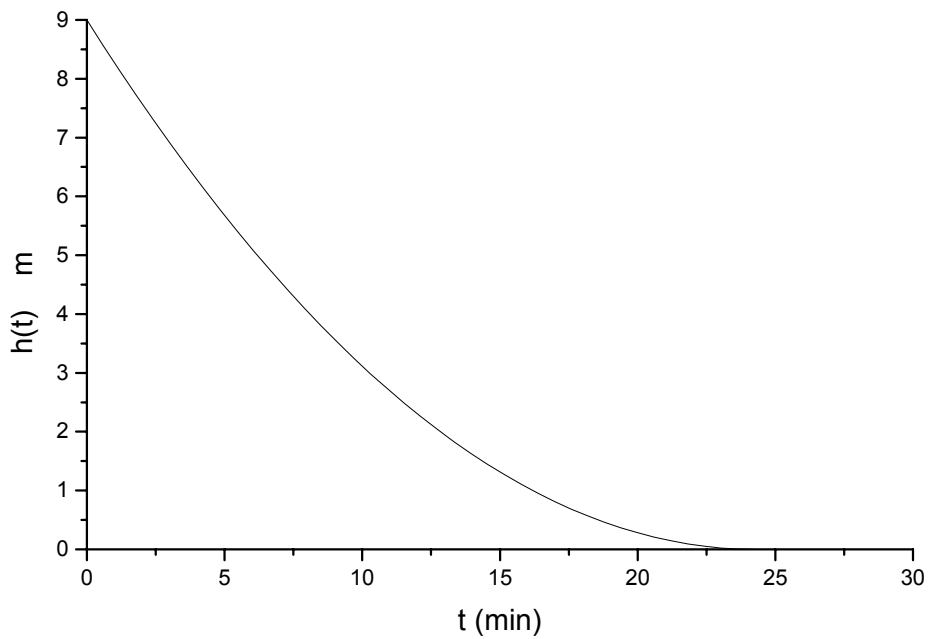


Fig. 9. Reactor pool draining. The water pool height is shown as function of time, following a complete rupture of a primary pipe of 10 inch in diameter.

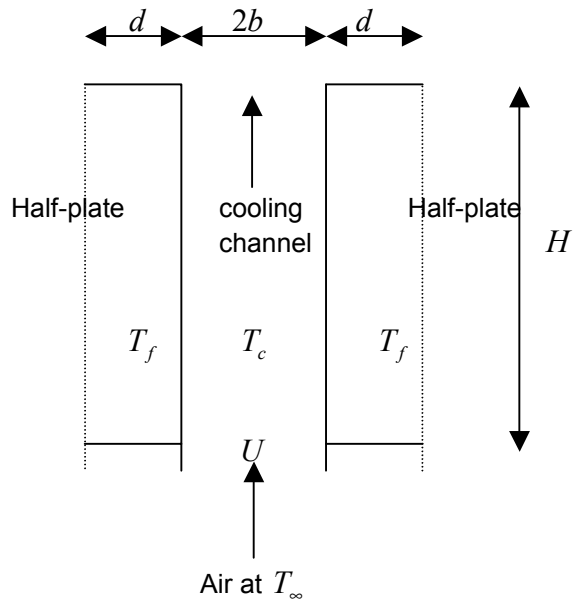


Fig. 10. Schematic of heat transfer model for cooling of reactor fuel plates through natural circulation of air.

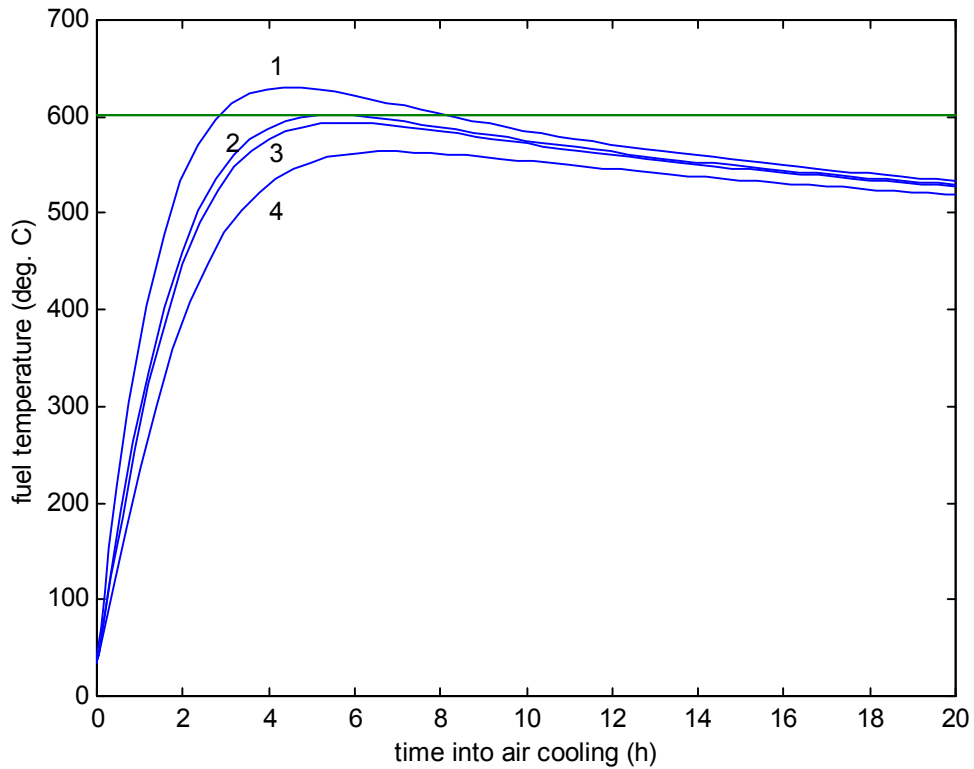


Fig. 11. Core cooling by natural convection in air. The fuel temperature is shown as function of time following a time lag of $t_{lg} = 16$ min (line 1), 1.5 h (line 2), 2 h (line 3) and 5 h (line 4). The horizontal line indicates the clad melting point.